Preliminary Study on the Crawler Unit of a Novel Self-Reconfigurable Hybrid Platform for Inspection

Sergio Leggieri[1,2], Carlo Canali[1], Ferdinando Cannella[1], Jinoh Lee[3], and Darwin G. Caldwell[1]

***Abstract*— Inspections of either industrial and civil structures are necessary to prevent damages and loss of human life. Although robotic inspection is gaining momentum, most of the operations are still performed by human workers. Many are the factors that slow down the spread of inspection robots, in particular, the lack of versatility as well as the low reliability of these devices constitute a huge limitation. In this work, we propose a design of a hybrid platform in the context of industrial inspection tasks. The aim is to address versatility issues exploiting modularity and self-reconfigurability. The final platform will consist of three main components: a main mobile base and two vehicles. All these systems would operate independently accomplishing specific inspection tasks. However, docking interfaces on each device will allow the systems to reconfigure into different robots extending the application range of each unit. The vehicles will work mainly in constrained environments and narrow spaces. The mobile base will monitor wide areas, carrying around the vehicles and deploying them near the inspection target. For dealing with challenging conditions, the two crawlers will dock together, reconfiguring into a snake-like robot. Docking to the main base, the two vehicle would act also as robotic arms, providing manipulation abilities to the system, thus allowing to perform maintenance operations as well. Still, the project is at an early stage of development. Revisions or adjustments on the prototype may follow the evaluations on the crawler performance.**

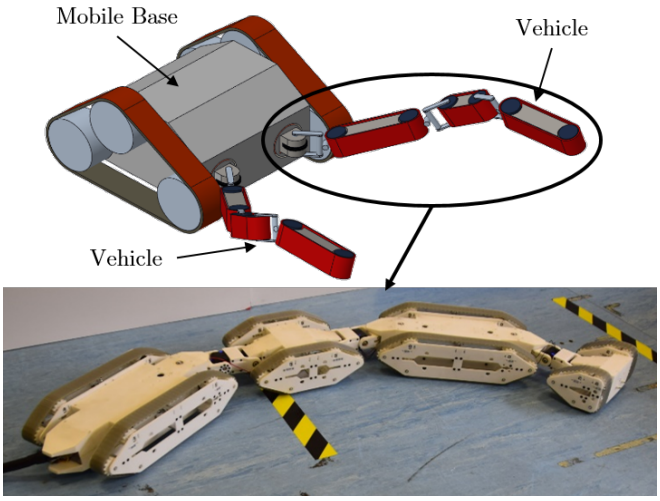

Fig. 1. On top, the representation of the hybrid platform: the main mobile base and two crawlers. On bottom, the first crawler prototype. The robot performs inspections in confined spaces. In challenging conditions, the vehicle connects with its twin or with the mobile base.

I. Introduction

Regular inspection and maintenance operations are crucial to ensure efficient and safe functioning of machines and structures, reporting issues before problems become critical. This is particularly true in industrial plants and civil infrastructures, where unexpected failures may lead to catastrophic events and potential loss of life. Nowadays, inspections are largely performed by humans and the most common operations involve data collection about target conditions using sensors and by visual assessment. Nonetheless, human-based inspections present many drawbacks, and even regular inspections may pose serious threats to workers, especially when the worker has to enter confined spaces.

Accordingly, there has been an increasing number of robots developed for inspections with the primary goal of minimizing such risks, simultaneously improving the reliability of results and reducing costs.Plant and pipe inspection robots assume particular relevance in this perspective. Here, inspection operations are often analogous and present many similar challenges: narrow spaces, small entrances, harsh environment, obstacles, etc. For these reasons, many common features can be identified in the designs of inspection systems.

Inspection robots can be mainly divided into two families according to the tasks: inspection of specific equipment and general inspection and monitoring. The former group includes highly specialized devices such as the robots shown in [1]–[3]. Typically, these robots exhibit a small-sized and target-oriented design, which confers them superior performance, but simultaneously reduces the versatility. Additionally, the deployment of these devices often requires the presence of a human operator in close proximity. During general inspections, the robots have to collect data on wide areas. These robots consist in autonomous or remotely operated mobile platforms equipped with sensors and fixed robotic arms [4]–[6]. Often, wheeled or tracked platforms are very big. However, these dimensions limit the overall robot mobility in tight corridors and narrow spaces. Slopes, obstacles and stairs are still an open challenge for such devices.

For inspecting pipes, robots have to traverse long distances as well but in highly constrained environments. The most common locomotion method is by wheels or tracks [7],

*This research was partly supported by ITECH R&D program of MOTIE/KEIT (No. 20014485 Development of small-size, high-precision and 500g-payload capable collaborative robot technology.)

[1]Authors are with the Department of Advanced Robotics, Istituto Italiano di Tecnologia, 16163 Genoa, Italy. sergio.leggieri@iit.it

[2]Author is with the Department of Engineer and Applied Science, University of Bergamo, Dalmine, Italy

[3]Author is with the Institute of Robotics and Mechatronics, German Aerospace Center (DLR), 82234 Weßling, Germany

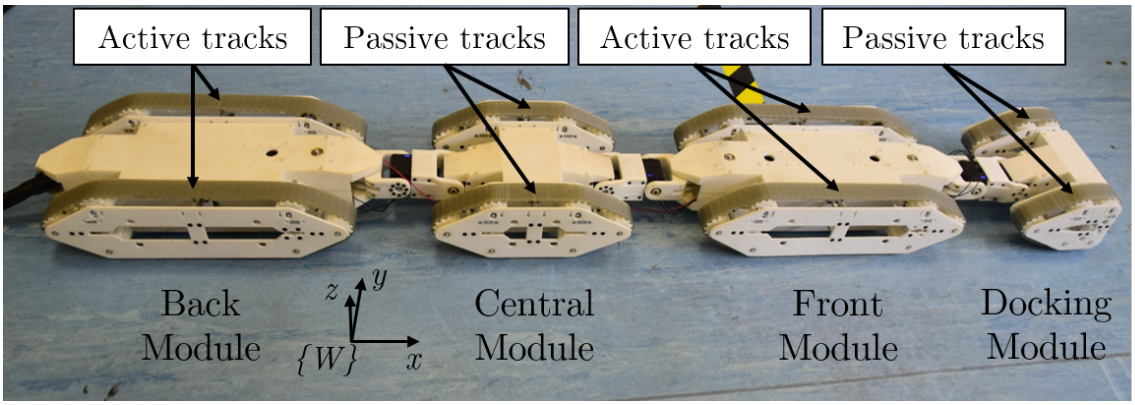

Fig. 2. The snapshot of the vehicle. $\{W\}$ is the inertial frame. From left to right: the back module, the central module, the front module and the docking module. Tracks on back and front modules are concurrently driven by two DC motors, one each. Tracks on central and docking modules are passive. Three kinematic chains connect all the modules and rotate the modules. All the modules have the same height and width. Front and Back modules are longer than central and docking module.

[8]. These robots consist of two or more modules and eventually equip complex mechanisms to fit and adapt to pipe networks, see for example [9]. Often, pipelines result from the combination of many segments and the systems with few modules can not adapt to it. Recently, the trend has shifted toward more complex and versatile robots with many modules, [8], such as snake robots, see [10]–[13].

These systems can move on and adapt to complex terrains, and propel either by using biological gaits [14], or by coordination of the body segments with scripted gaits [15]. The slender body makes snake robots extremely suitable for inspections in constrained environments, as discussed in [16]–[18].

Self-reconfigurability represents an interesting trade-off for combining small and easy to control systems into articulated robots capable of adapting to many scenarios, see [19], [20]. Chain structured systems perform search and rescue or exploration missions which are similar to many inspection scenarios, see examples in [21]–[24].

In this paper, the idea is to exploit modularity and self-reconfigurability to design a versatile multi-purpose hybrid platform which will consist of three systems: a mobile main base and two twins vehicles, as shown in Fig. 1. These units are designed to perform inspections independently or in collaboration. In particular, the two vehicles are especially suitable for inspection in constrained environments and narrow spaces. Instead, the mobile base is more useful in patrolling and monitoring of wide areas. If the targets or the surroundings are too big or challenging for single units, the systems can reconfigure autonomously without human intervention. For example, the crawlers can dock together forming a snake robot for climbing stairs or overcoming obstacles. Otherwise, the crawlers can couple with the mobile base turning the hybrid platform into a dual arm system that can execute manipulation and maintenance tasks. In such configuration, the mobile base becomes a carrier which can deploy and recover the vehicles near their inspection site. This work will focus on the design features of the vehicles and the ground maneuverability of these crawlers.

The rest of the paper is organized as follows: Section II offers a general summary of the crawler and detailed descriptions of main mechanical components. Section III provides the experimental results obtained by the robot performing different types of motions. Section IV provides conclusive considerations and future works.

II. Crawler Description

The vehicle consists of three main modules plus the docking module, see Fig. 2. Each module is connected with the others through active joints. In particular, such joints are arranged in three kinematic chains, which consist of a pitch joint, namely a joint with its rotation axis aligned with the y axis of the inertial frame $\{W\}$, and the equivalent of a Cardan joint, namely a joint with two rotation axis parallel to the y and z axis of $\{W\}$, respectively. The system results redundant either in kinematics and actuation. Kinematic redundancy confers great adaptability to different terrains and obstacles, which is crucial when the crawler operates in unknown environments. Actuation redundancy ensures an additional degree of fault-tolerance and reliability to the system.

The track blocks on the two longest modules are active, while the others are passive. Single DC motor concurrently drives the tracks on both sides of active modules. The docking module allows autonomous mechanical coupling between two vehicles. In this way, the system re-configures into a snake robot or connects to the main base.

A. Track Design

The robot has three types of track blocks. Each block covers almost entirely the corresponding module sides. The docking module has a different layout since it has to couple to the other systems. Here, we focus on the active blocks as most representative, the passive blocks have almost the same features.

Referring to Fig. 3, two parallel plates enclose the track system, four supporting girders and pulley shafts connect these plates into a rigid frame. The left and right track

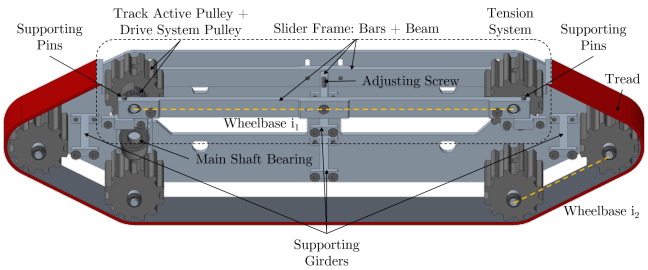

Fig. 3. The CAD drawing of the active track block at the right side, where the active pulley is flanked by the output pulley of the drive system. The tread wraps around six pulley and the top pulleys belong to the tension system frame, which slides along four supporting pins. The tread tension can be adjusted through an adjusting screw. (The internal plate is omitted to display the track block features.)

systems are mirrored, both the two internal plates connect the track systems to the crawler chassis. The external plates house the bearings that support the main shaft of the drive system. Each track system has six timing pulleys over which the tread is wrapped. The pulley that actively drives the track is shorter than the others because it is flanked by the last stage pulley of the drive system. The pulleys are arranged in a hexagonal shape, therefore the track block has a slender layout to possibly remove or overcome debris stuck between modules.

The tension system is an adjustable mechanical slider which consists of two bars connected by a perpendicular beam, which has a through hole in the middle. The tension system is forced to slide along the vertical direction by four pins, one for each vertex, mounted on each side of the track plates.

Using geometrical considerations and trigonometric formulas, it is possible to verify the belt length as follows:

$$L = 2i_1 + 4i_2 + 2\pi r \left(4\frac{\alpha}{360} + 2\frac{2\beta}{360}\right), \qquad (1)$$

where i_1 is the distance between the top and bottom pair of pulleys, and i_2 is the diagonal wheelbase between the other pulleys, as also seen in Fig. 3. The pulley pitch radius is denoted by r. The wrapping angle around the four parallel pulleys is α, while β is half the wrapping angle around the front and rear pulleys.

B. Drive system

Both the active tracks of each active module are driven concurrently by a single DC motor, which is placed in the middle of the vehicle chassis. The drive system is a two stage transmission with $1:1$ reduction ratio, and it transfers motion to the track systems. Referring to Fig. 4, the first stage consists of the timing belt that connects the pulley on the DC motor output shaft to the pulley on the main shaft. The first stage is completely enclosed in the crawler chassis, preventing unexpected transmission failure due to debris. The drive system second stage consists of two timing belts, which wrap around two pulleys, sideways on the main shafts, and the output pulleys. The second stage belts are protected by the track plates, so to avoid damages from debris.

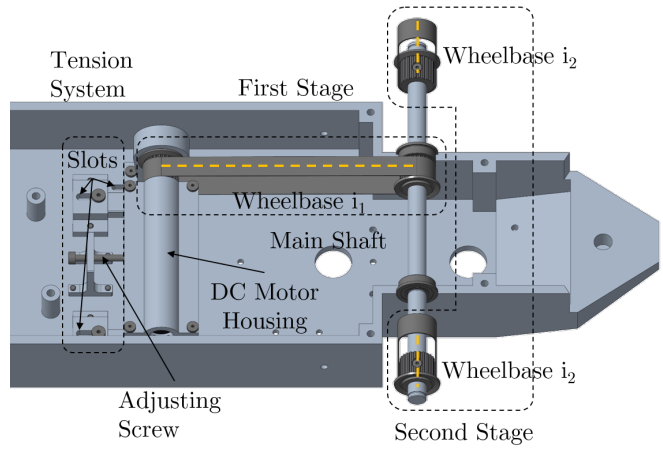

Fig. 4. The CAD drawing of the drive system: at the first stage, the belt transmits the rotation of the DC motor to the main shaft; and at the second stage, two pulleys on the main shaft transfer the motion to the output pulleys connected to the track blocks. The wheelbase i_1 is tuned with an adjusting screw and the motor housing is anchored to the vehicle hull.

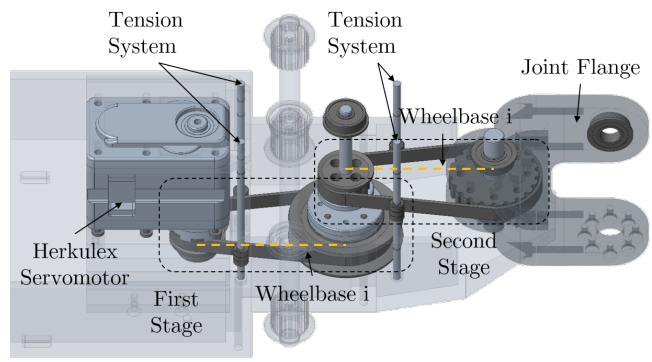

Fig. 5. The CAD drawing of the yaw joint: at the first stage, the belt connects the servomotor pulley to the biggest pulley on first shaft, while at the second stage, the small pulley on the first shaft transmits rotation to the biggest pulley on which the joint flange is fixed, where the fixed tension systems tighten each belt on both sides.

In order to tighten the first stage transmission belt, the DC motor is fixed on a sliding element whose position is adjustable. In the bottom part of the motor housing, four fixing points match four slots in the vehicle chassis. The motor housing has two additional fixing point within the vehicle hull. The second stage belts are tightened by the same tension system used for the tracks.

C. Yaw joint

The yaw joints are responsible for steering the vehicle. When the vehicle couples with its twin, these joints will produce the typical undulating motion of snake robots. For these reasons, such joints require a high torque for winning the friction forces on tracks. Therefore, a dual stage transmission has been designed in order to increase the output torque of each servomotor, as shown in Fig. 5. Such transmission has the same ratio in between stages and the total reduction ratio is $3.83:1$.

Due to the narrow spaces in vehicle chassis terminal parts, the adopted solution foresees fixed tension systems

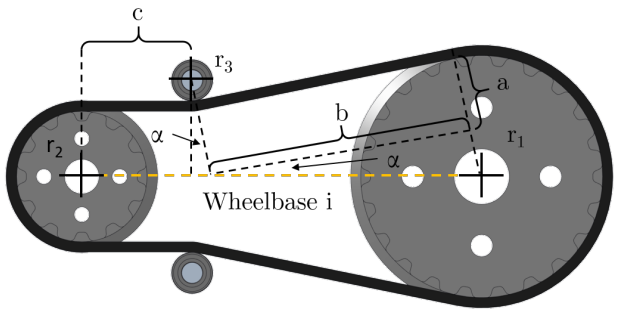

Fig. 6. Yaw joint transmission stage. The idlers have radii r_3. The input pulley radius is r_2 and the output pulley radius is r_1. The orange dashed line represents the wheelbase i. The tentative position of idlers is denoted by c. Solving the system in (3) and (2), it is possible to compute the final belt length.

TABLE I
CRAWLER TECHNICAL SPECIFICATIONS

Herkulex Servomotor	Model: DRS-0602 Total weight: 145g Total Stall Torque: 7.6Nm Reduction Ratio: 202:1
Maxon Motor	Model: DCX12L Total weight: 36.6g Total Stall Torque: 0.99Nm Reduction Ratio: 83:1
Arduino Board	Model: Mega 2560 Microcontroller: ATmega 2560 Clock Speed: 16MHz
L298N Motor Driver	Driver: L298N Dual H Bridge Motor Channels: 2 Driver Voltage: 5-35V

consisting of external idlers on each belt side. Once the wheelbase i of each transmission stage is determined, the desired position for the idlers is chosen in such a way that the resulting belt length matches the commercial timing belt length. Such length is calculated as follows:

$$L = \pi r_2 + 2c + 2\pi r_3 2\frac{\alpha}{360} + 2b + 2\pi r_1 \frac{(2\alpha + 180)}{360}, \quad (2)$$

where r_1 and r_2 are the pitch radii of the small and the big pulley, respectively. The idler radius is r_3 and c is the distance between the centers of the smallest transmission pulley and the idler, respectively. The segment tangent to both the idler and the biggest pulley is b, and α is the wrap angle of the belt on the idlers. It is intuitive that α, b and c are dependent. As shown in Fig. 6, for a desired distance c, it is possible to find the other parameters solving the following trigonometric equations:

$$\begin{cases} b\tan\alpha + a = r_1 \\ (r_3 + a)\cos\alpha = r_2 + r_3 \\ (r_3 + a)\sin\alpha + \frac{b}{\cos\alpha} + c = i \end{cases} \quad (3)$$

where, a is the segment between the idler tangent point and the wheelbase identified by the straight line passing through the idler center and the belt tangent point on the idler.

On the yaw joint it is fixed the joint flange, which directly connects the successive pitch joint. Due to the proximity of the two perpendicular rotation axis, such configuration can be considered as an active Cardan joint.

D. Technical Aspects

Referring to Fig. 2, all the modules have the same height and width, but they differ slightly in length. The track height is 108mm, and the modules are 218mm wide. The back and the front modules are 440mm long, while the central module plus the pitch joints are 347mm long in total.

The back module encloses the Herkulex DRS-0602 servomotor and the DCX12L Maxon Motor, see table I. The back module houses also the electronic boards: the microcontroller and the motor drivers, see table I. The central module contains two servomotors and has additional free space for payloads and sensors. The front module includes two servomotors and the other DC Motor. The docking module houses one servomotor, the docking mechanism and another motor driver. At the moment, the vehicle is powered through an umbilical cable connected to an external power supply and to a computer. A dual axis joystick is used to control the crawler remotely.

III. EXPERIMENTAL TESTS AND RESULTS

The vehicle ground maneuverability has been tested during lab experiments. The aims of such experiments are twofold. On one side, functionality of all the subsystems described is verified. On the other side, the crawler performance and its maneuverability are evaluated experimentally in common scenarios that can be met during inspections. The results are discussed in each subsection. If not differently specified, all the pitch joints are controlled to keep a zero angle between modules during the experiments.

A. Forward motion & Overcoming ditches

First of all, the vehicle is tested in performing forward and backward motion on flat terrain. The system travels a distance of 1 meter in 10 seconds, achieving a speed of about 0.1m/s. Then, the crawler is tested while moving over a ditch. Note that, the gap traversed is longer than the length of each module. Thanks to the active joints, the robot succeeds in traversing a 0.5m gap, as shown in Fig. 7. Although the timing belts provide enough friction with the ground in active modules to propel the vehicle, the friction on the passive modules is not sufficient to win internal frictions in passive track systems. However, this represents a minor issue which can be solved by applying more adhesive rubber strips on the external side of each belt.

B. Turning motion

Since the active tracks of each active module are concurrently driven by a single motor, the vehicle can not turn using a skid-steering technique. For turning the robot, the yaw joints have to rotate the modules while the active tracks spin, see Fig. 8. Due to the high torques produced by the yaw joints, the robot can rotate the modules assuming

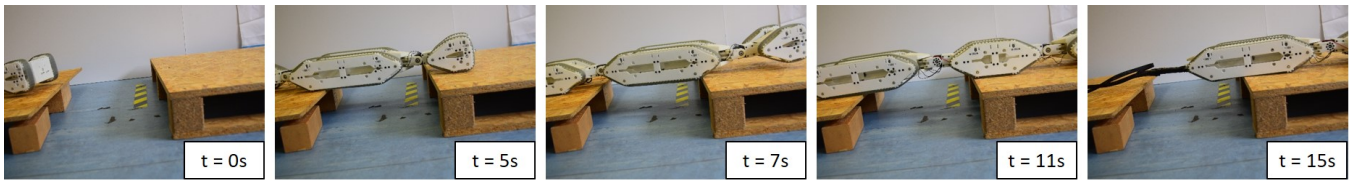

Fig. 7. The sequence of the crawler moving forward over a 0.5m ditch with a longitudinal velocity of approximately 0.1m/s.

a C-configuration even if stationary. Considering uniform velocities and constant joint angles on each module, it is possible to estimate the curvature radius using the formula:

$$r = \frac{l_2 + l_1 \cos q_y}{\sin q_y}, \tag{4}$$

where q_y is the joint angle, l_1 and l_2 are the front and central module half lengths, respectively. It is worth to mention that, the length l_2 can be reduced by controlling the robot pitch joints, in such a way that the central module is raised above the ground. The crawler rotates of about 90 degrees in 20 seconds, with all yaw joints at their maximum allowed rotation of 50 degrees.

C. Turning on the spot

The crawler can also turn on the spot. This is a useful feature especially in constrained environments or to make little adjustments to the vehicle heading. To turn on the spot, the yaw joints rotate the modules in a S-configuration while the vehicle is stationary, as in Fig. 8. Then, the two active motors spin the tracks in opposite directions. Given the track linear velocity v, the angular velocity ω of the central module is given as follows:

$$\omega = \frac{v \sin q_y}{l_2}, \tag{5}$$

where q_y is the joint angle, l_2 is the central module half length. Also in this case, reducing the length l_2 by lifting the central module will increase the robot angular velocity ω. The central module rotates of ± 90 degrees in 32 seconds.

D. Climbing ramp

The robot succeeds in climbing and descending ramps, as shown in Fig. 9. The crawler is tested on slopes up to $20°$, over this value, the friction on tracks is not enough to push the vehicle and the tracks start to slip on the ground. During this experiment, the docking module is lifted above the ground to help the vehicle to climb the initial ramp step. The vehicle travels 0.2 meters in 12 seconds. As mentioned in previous subsection, adding more adhesive strips on the tracks external surface should allow to climb steeper slopes.

E. Moving on uneven terrains

The crawler can move on uneven terrain, see Fig. 9. During this experiment, all the pitch joints are passive except for those connecting the front module to the docking module. In this way, three out four modules adapt to the terrain, while the docking module weight slightly increases the friction force of the front module. The robot successfully traverses the 2 meter long terrain in 30 seconds. If the vehicle gets stuck it is possible to rotate the modules and recover. Even if the passivity of pitch joints can be very useful in descending transitions of terrain, it reduces the overall crawler maneuverability. For this reason, future work will focus on integrating an additional dual axis joystick or even on designing multi-input controller to provide the user the full control over the robot.

IV. Conclusion

Inspection robotics is an active research field. Most of the inspection operations consist in reaching target, collecting data from sensors and providing visual feedback to the operator. However, inspection robots often lack in adaptability and versatility even if they posses all the equipment.

In this paper, we propose a novel modular hybrid platform for inspection which exploits self-reconfigurability and modularity for adapting to many inspection missions. The platform consists of two modular vehicles and a mobile main base. Here, we focused on the crawler design and we described the most important features. The vehicle ground maneuverability has been tested and the results discussed. The robot achieved a forward velocity of 0.1m/s on flat terrain. Thanks to its structure, the crawler successfully overcame a 0.5m gap. The vehicle was able to perform turning motion and succeeded in turning on the spot. Moreover, the system was tested in climbing ramps up to 20 degrees slope and in moving over uneven terrain. During these experiments, some minor issues were identified, such as the low friction on the tracks, and will be addressed in future works. Moreover, future works will focus on testing the entire crawler kinematics evaluating the spatial maneuverability of the system. Next steps will also involve the experiments on the two vehicles in snake configuration. Finally, the design of the mobile main base will be finalized and the hybrid platform performance will be evaluated.

References

[1] E. Zwicker, W. Zesch, and R. Moser, "A modular inspection robot platform for power plant applicationst," in *2010 1st International Conference on Applied Robotics for the Power Industry*, Oct. 2010, pp. 1–6.

[2] G. Caprari *et al.*, "Highly compact robots for inspection of power plants," *Journal of Field Robotics*, vol. 29, pp. 47–68, Gen. 2012.

[3] A. Pistone *et al.*, "Reconfigurable inspection robot for industrial applications," *Procedia Manufacturing*, vol. 38, pp. 597 – 604, 2019.

[4] J. Steele *et al.*, "Development of an Oil and Gas Refinery Inspection Robot," *ASME International Mechanical Engineering Congress and Exposition, Proceedings (IMECE)*, vol. 4, pp. 1–10, Nov. 2014.

[5] I. Maurtua *et al.*, "MAINBOT – Mobile Robots for Inspection and Maintenance in Extensive Industrial Plants," *Energy Procedia*, vol. 49, pp. 1810–1819, 2014.

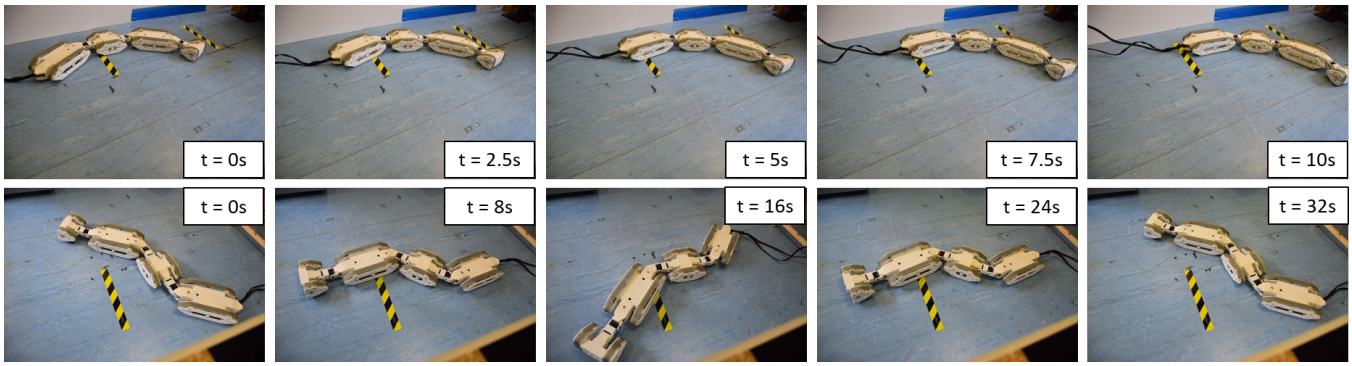

Fig. 8. Turning motion sequences. In the top sequence, the crawler bends the modules assuming a C-configuration and performs turning motion. It turns 45 degrees in 10 seconds. In the bottom sequence, the vehicle adopts the S-configuration and turns on the spot. It rotates ± 90 degrees in 32 seconds

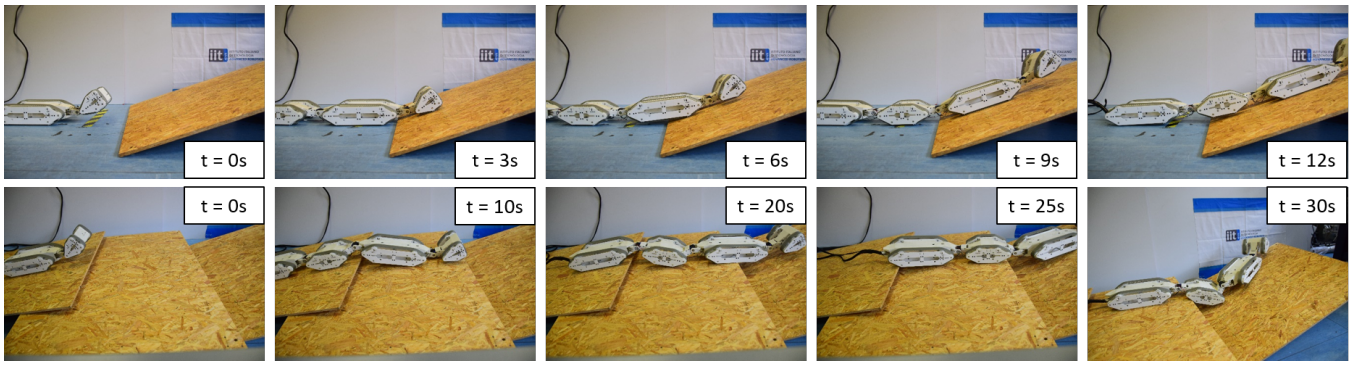

Fig. 9. Climbing ramp and moving on uneven terrain sequences. In the top sequence, the robot climbs a 200mm ramp, with 20° slope, in about 12 seconds. In the bottom sequence, the crawler moves on uneven terrain. It traverses the 2 meters long terrain in about 30 seconds.

[6] S. Soldan, J. Welle, T. Barz, A. Kroll, and D. Schulz, *Towards Autonomous Robotic Systems for Remote Gas Leak Detection and Localization in Industrial Environments*. Springer Tracts in Advanced Robotics, Springer, Berlin, Heidelberg, Jan. 2014, pp. 233–247, in Yoshida, K. and Tadokoro, S., Field and Service Robotics, ISBN: 978-3-642-40685-0.

[7] J. Mirats-Tur and W. Garthwaite, "Robotic Devices for Water Main In-Pipe Inspection: A Survey," *Journal of Field Robotics*, vol. 27, pp. 491–508, Jul. 2010.

[8] G. Mills, A. Jackson, and R. Richardson, "Advances in the Inspection of Unpiggable Pipelines," *Robotics*, vol. 6, p. 36, Nov. 2017.

[9] J. Park, D. Hyun, W. Cho, T. Kim, and H. Yang, "Normal-Force Control for an In-Pipe Robot According to the Inclination of Pipelines," *IEEE Transactions on Industrial Electronics*, vol. 58, pp. 5304–5310, Dec. 2011.

[10] S. Hirose, "Snake-like locomotors and manipulators," *Biologiclly Inspired Robots*, 1993.

[11] M. Mori and S. Hirose, "Development of active cord mechanism ACM-R3 with agile 3D mobility," in *Proceedings 2001 IEEE/RSJ International Conference on Intelligent Robots and Systems. Expanding the Societal Role of Robotics in the Next Millennium (Cat. No.01CH37180*, Mar. 2001, pp. 1552–1557.

[12] C. Wright *et al.*, "Design and architecture of the unified modular snake robot," in *2012 IEEE International Conference on Robotics and Automation*, May 2012, pp. 4347–4354.

[13] P. Liljebäck, K. Y. Pettersen, and Ø. Stavdahl, "A snake robot with a contact force measurement system for obstacle-aided locomotion," in *2010 IEEE International Conference on Robotics and Automation*, Jun. 2010, pp. 683–690.

[14] S. Hirose and M. Mori, "Biologically Inspired Snake-like Robots," in *2004 IEEE International Conference on Robotics and Biomimetics*, Sep. 2004, pp. 1–7.

[15] M. Tesch *et al.*, "Parameterized and scripted gaits for modular snake robots," *Advanced Robotics*, vol. 23, no. 9, pp. 1131–1158, 2009.

[16] H. Schempf *et al.*, "Visual and nondestructive evaluation inspection of live gas mains using the Explorer™ family of pipe robots," *Journal of Field Robotics*, vol. 27, pp. 217–249, May 2010.

[17] J. Borenstein, M. Hansen, and A. Borrell, "The OmniTread OT-4 Serpentine Robot 1 – Design and Performance," *Journal of Field Robotics*, vol. 24, pp. 601–621, Jul. 2007.

[18] S. A. Fjerdingen, P. Liljebäck, and A. A. Transeth, "A snake-like robot for internal inspection of complex pipe structures (PIKo)," in *2009 IEEE/RSJ International Conference on Intelligent Robots and Systems*, Oct. 2009, pp. 5665–5671.

[19] J. Liu, X. Zhang, and G. Hao, "Survey on Research and Development of Reconfigurable Modular Robots," *Advances in Mechanical Engineering*, vol. 8, pp. 1–21, Aug. 2016.

[20] S. Chennareddy, A. Agrawal, and A. Karuppiah, "Modular Self-Reconfigurable Robotic Systems: A Survey on Hardware Architectures," *Journal of Robotics*, vol. 2017, pp. 1–19, Mar. 2017.

[21] H. Zhang, G. Zong, and Z. Deng, *A Reconfigurable Mobile Robots System Based on Parallel Mechanism*. IntechOpen, Apr. 2008, chapter 16, pp. 347–362, in Wu, H., Parallel Manipulators, towards New Applications, ISBN: 978-3-902613-40-0.

[22] W. Wei and T. Huilin, "Reconfigurable multi-robot system kinematic modeling and motion planning," in *2011 6th IEEE Conference on Industrial Electronics and Applications*, Jun. 2011, pp. 1672–1677.

[23] H. B. Brown, J. M. Vande Weghe, C. A. Bererton, and P. K. Khosla, "Millibot trains for enhanced mobility," *IEEE/ASME Transactions on Mechatronics*, vol. 7, no. 4, pp. 452–461, Dec. 2002.

[24] P. Ben-Tzvi, A. A. Goldenberg, and J. Zu, "Design and Analysis of a Hybrid Mobile Robot Mechanism With Compounded Locomotion and Manipulation Capability," *Journal of Mechanical Design*, vol. 130, Jul. 2008.